

DETC2003/MECH-48356

RECONSTRUCTION OF THE DYNAMIC RAIL-WHEEL CONTACT FORCES

Svenja Kirchenkamp *, **Dirk Söffker**
 Dynamics and Control, University Duisburg-Essen
 47048 Duisburg, Germany
 Email: svenja.kirchenkamp@uni-duisburg.de,
 soeffker@uni-duisburg.de

ABSTRACT

This contribution introduces a virtual measurement device for the reconstruction of the in practice unmeasurable rail-wheel contact forces. For this aim the Proportional-Integral (PI)-Observer is used. Then, the concept of a measurement sleeve at the axle bearing is shown. With the displacement measurements resulting from the sleeve using the PI-Observer, an estimation of the tangential contact force and the dynamic normal force is possible. Using the simulation of the rail-wheel contact, the feasibility of the estimation of the contact force behavior is shown. As an outlook for further applications of the PI-Observer in the context of rail-wheel contact force estimation, the reconstruction of contact forces by using acceleration measurements is demonstrated by an example of an elastic beam for the first time.

INTRODUCTION

The adhesion-friction micromechanism is the core of the transport mechanism of locomotions. The rail-wheel contact is highly nonlinear due to the complex geometrical contact problem and the unknown environmental parameters (temperature etc.). Furthermore, the interaction between the elastic track, the elastic rail, the elastic contact itself and the wheel is of interest because of several safety, economical and comfort aspects [1]. The problem is unavailable measurements within the contact area. The PI-Observer technique offers a possibility for getting 'measurements' in cases where real measurements are impossi-

ble or too costly. The PI-Observer uses known model parts and easy available measurements from the known parts to estimate unknown effects within unknown parts of a system using inner connections of a system to replace real measurements by virtual measurements based on easy-to-realize measurements.

The idea of this 'virtual measurement device' method is illustrated in Fig. 1.

The use of a measurement sleeve at the axle bearing is a possibility of getting measurements from the rotating wheelset without complicated wiring and resulting wear.

Future applications of this measurement device are the drive control or the control of single-wheel drives. With this applications it is possible to optimize the contact behavior of the rail-wheel contact which can reduce the wear.

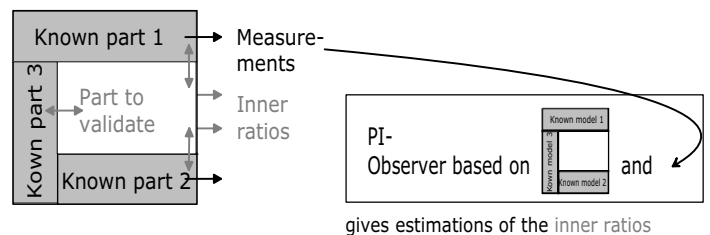


Figure 1. THE PI-OBSERVER AS A VIRTUAL MEASUREMENT DEVICE

*Address all correspondence to this author.

THE PROPORTIONAL-INTEGRAL-OBSERVER

The Luenberger observer is based on the following system description

$$\dot{x} = Ax + Bu, \quad y = Cx \quad (1)$$

with the state vector x of order n , the vector of measurements y of order r_1 and the known input vector u of order m . The system matrix A , the input matrix B and the output matrix C are of appropriate dimensions. This conventional observer gives under specific conditions (observability) an estimation \hat{x} of the state vector.

The applied PI-Observer [2] is based on the following description:

$$\dot{x} = Ax + Bu + N_1 f(x, u, t), \quad y = Cx. \quad (2)$$

The vector function $f(x, u, t)$ describes the nonlinearities caused by the external input, unknown inputs and unmodeled dynamics of the plant and may be a nonlinear function of states, control inputs and time. The matrix N_1 locates the unknown external influences to the system states. The vector of nonlinearities is approximated by

$$f \approx Hv \quad (3)$$

This approximation is already used successfully in several practical and theoretical applications concerning machine diagnosis [3] and also observer-based control [4, 5].

In the theory of Disturbance Rejection Control (DRC) [6–8], the linear time-invariant system with the unknown inputs $N_1 f$ caused by nonlinearities are described by the linear exo-system

$$\dot{v} = Fv \quad (4)$$

giving the unknown inputs or unmodeled dynamics.

These states do not necessarily represent velocities. They represent also angles, accelerations etc. depending on the states of the vector \dot{x} .

This results in the extended linear system

$$\begin{bmatrix} \dot{x} \\ \dot{v} \end{bmatrix} = \begin{bmatrix} A & N_1 H \\ 0 & F \end{bmatrix} \begin{bmatrix} x \\ v \end{bmatrix} + \begin{bmatrix} B \\ 0 \end{bmatrix} u, \quad (5)$$

$$y = \begin{bmatrix} C & 0 \end{bmatrix} \begin{bmatrix} x \\ v \end{bmatrix}, \quad (6)$$

which can be used as an extended base for developing a classical linear observer.

In the applications [3–5] it is noticed that using

$$F = 0, \quad F \rightarrow 0 \quad (7)$$

leads to a very good reconstruction of the diagnosed nonlinearity.

By the given procedure using ' $F = 0$ ' in the sense of disturbance model philosophy, the successfully applied scheme appears as the PI-observer and will be seen as a natural comprehensible extension of the well known Luenberger observer [9].

Figure 2 shows the structure of the observer and therefore, (2) is written in the following form

$$\dot{x} = Ax + Bu + b + N^* n^*(x, t). \quad (8)$$

where b is the known input which is independent from u and $N^* n^*$ describes the unknown, external inputs.

Here in contrast to the conventional Luenberger approach a second loop with two gain matrices L_2, L_3 and an integrator is used additionally.

Now, the question is how to determine the matrices L_1, L_2 and L_3 such that the corresponding PIO works well. Therefore the estimation performance is analyzed for different cases of the dynamical behavior of the unknown input related to the nominal system.

Estimation Behavior

The development of the theory behind, follows the works in [9], [2]. From the structure of the PI-observer depicted in Fig. 2 it follows that the dynamics of PI-observer is described by

$$\dot{\hat{x}} = A\hat{x} + L_3 \hat{f} + Bu + L_1 (y - \hat{y}) \quad \dot{\hat{f}} = L_2 (y - \hat{y}) \quad (9)$$

where $\hat{y} = C\hat{x}$. Writing (2) in a matrix form gives

$$\begin{bmatrix} \dot{\hat{x}} \\ \dot{\hat{f}} \end{bmatrix} = \begin{bmatrix} A & L_3 \\ 0 & 0 \end{bmatrix} \begin{bmatrix} \hat{x} \\ \hat{f} \end{bmatrix} + \begin{bmatrix} B \\ 0 \end{bmatrix} u + \begin{bmatrix} L_1 \\ L_2 \end{bmatrix} (y - \hat{y}) \quad (10)$$

or

$$\begin{bmatrix} \dot{\hat{x}} \\ \dot{\hat{f}} \end{bmatrix} = \underbrace{\begin{bmatrix} A - L_1 C & L_3 \\ -L_2 C & 0 \end{bmatrix}}_{A_e} \begin{bmatrix} \hat{x} \\ \hat{f} \end{bmatrix} + \begin{bmatrix} B \\ 0 \end{bmatrix} u + \begin{bmatrix} L_1 \\ L_2 \end{bmatrix} y. \quad (11)$$

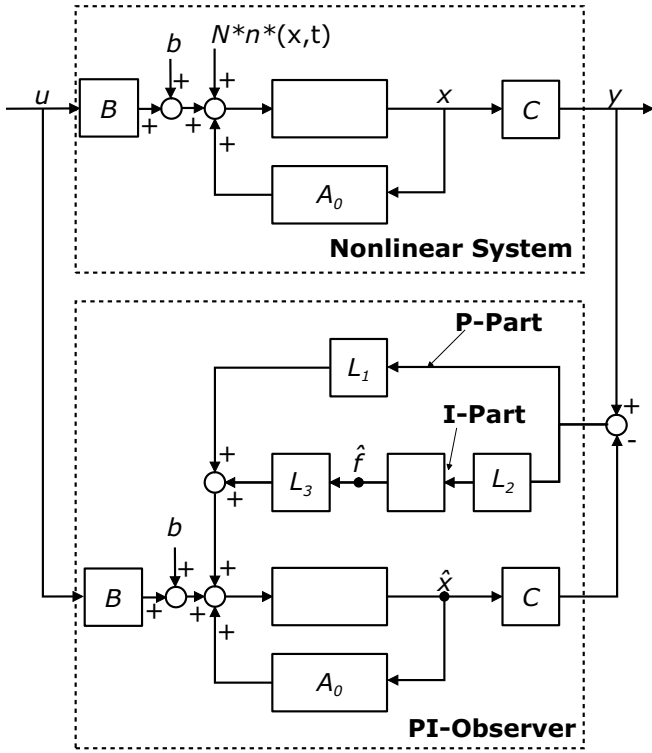


Figure 2. STRUCTURE OF THE PI-OBSERVER

Now the question is how to design the gain matrices L_1 , L_2 , and L_3 , such that the observer can estimate approximately the states x of the plant in presence of the unknown input Nn . The estimation error is defined as $e(t) = \hat{x}(t) - x(t)$. Then, from (1), (2) and (11),

$$\begin{bmatrix} \dot{e} \\ \dot{\hat{f}} \end{bmatrix} = A_e \begin{bmatrix} e \\ \hat{f} \end{bmatrix} \quad (12)$$

results for the case of system (1), or

$$\begin{bmatrix} \dot{e} \\ \dot{\hat{f}} \end{bmatrix} = A_e \begin{bmatrix} e \\ \hat{f} \end{bmatrix} - \begin{bmatrix} N_1 \\ 0 \end{bmatrix} f \quad (13)$$

results for the case of system (2) with unknown inputs or nonlinearities. From (11) the following result can be obtained [9].

Known System Without External Inputs

Theorem 1. If the pair (A, C) is observable, then there exists a PI-observer with any dynamics for the system (1), such that $\lim_{t \rightarrow \infty} [\hat{x}(t) - x(t)] = 0$ for any initial states $x(0)$, $\hat{x}(0)$ and $\hat{f}(0)$.

Proof. From the dynamics (11) of PI-observer it can be seen that the dynamics or poles of (11) can be arbitrarily assigned if and only if the matrix pair $\left(\begin{bmatrix} A & L_3 \\ 0 & 0 \end{bmatrix}, [C \ 0] \right)$ is observable, i.e.

$$\text{rank} \left\{ \begin{bmatrix} sI - A & -L_3 \\ 0 & sI \\ C & 0 \end{bmatrix} \right\} = n + \dim(\hat{f}) \quad (14)$$

holds for all $s \in \mathbf{C}$. Furthermore, the condition (13) is equivalent to

$$\text{rank} \left\{ \begin{bmatrix} A & L_3 \\ C & 0 \end{bmatrix} \right\} = n + \dim(\hat{f}) \quad (15)$$

when $s = 0$ and

$$\text{rank} \left\{ \begin{bmatrix} sI - A \\ C \end{bmatrix} \right\} = n \quad (16)$$

when $s \neq 0$. The condition (15) implies that the dimension of the integrator must be less than or equal to that of the outputs. Since the matrix L_3 may be arbitrarily selected, the rank condition (16) holds if and only if

$$\text{rank} \left\{ \begin{bmatrix} A \\ C \end{bmatrix} \right\} = n \quad (17)$$

Combining the conditions (16) and (17) leads to

$$\text{rank} \left\{ \begin{bmatrix} sI - A \\ C \end{bmatrix} \right\} = n \quad (18)$$

for all $s \in \mathbf{C}$, i.e. (A, C) is observable.

A main motivation to study the PI-observer is to reconstruct the states of the system (2) with nonlinearities. The following two theorems give the results in case of the system (2).

Known Systems with Constant External Inputs

Theorem 2. Assume that $\lim_{t \rightarrow \infty} f(x, u, t)$ exists. Then, there exists a PI-observer with any dynamics for the system (2), such that $\lim_{t \rightarrow \infty} [\hat{x}(t) - x(t)] = 0$ for any initial states $x(0)$, $\hat{x}(0)$ and $\hat{f}(0)$ if (A, C) is observable and

$$\text{rank} \left\{ \begin{bmatrix} A & N_1 \\ C & 0 \end{bmatrix} \right\} = n + r_1 \quad (19)$$

Proof. Using the construction method, we prove Theorem 2. Let $L_3 = N_1$. Then, the dynamics (13) of the estimation error of PI-observer (11) becomes

$$\begin{bmatrix} \dot{e} \\ \dot{\hat{f}} \end{bmatrix} = A_e \left\{ \begin{bmatrix} e \\ \hat{f} \end{bmatrix} - \begin{bmatrix} 0 \\ I \end{bmatrix} f \right\} \quad (20)$$

where $A_e = \begin{bmatrix} A - L_1 C & N_1 \\ -L_2 C & 0 \end{bmatrix}$. Similarly with the proof of Theorem 1, the eigenvalues of the matrix A_e can be arbitrarily assigned by the matrices L_1 and L_2 if and only if the matrix pair $\left(\begin{bmatrix} A & N_1 \\ 0 & 0 \end{bmatrix}, [C \ 0] \right)$ is observable, i.e.

$$\text{rank} \left\{ \begin{bmatrix} sI - A & -N_1 \\ 0 & sI \\ C & 0 \end{bmatrix} \right\} = n + r_1 \quad (21)$$

holds for all $s \in \mathbb{C}$. This condition is equivalent to

$$\text{rank} \left\{ \begin{bmatrix} A & N_1 \\ C & 0 \end{bmatrix} \right\} = n + r_1 \quad (22)$$

when $s = 0$ and

$$\text{rank} \left\{ \begin{bmatrix} sI - A \\ C \end{bmatrix} \right\} = n \quad (23)$$

when $s \neq 0$. This implies that under the conditions in Theorem 2 the dynamics of PI-observer (10) for the system (2) can be arbitrarily assigned. Therefore, the eigenvalues of A_e can be arbitrarily placed at any locations in the left-half complex plane when the conditions in Theorem 2 are fulfilled. This means that the dynamics (20) can be stabilized by means of the matrices L_1 and L_2 . When the dynamics (20) is asymptotically stable, its solution will converge to the equilibrium. Then, from (20) it can be easily seen that

$$\lim_{t \rightarrow \infty} \begin{bmatrix} e(t) \\ \hat{f}(t) \end{bmatrix} = \begin{bmatrix} 0 \\ \lim_{t \rightarrow \infty} f(x, u, t) \end{bmatrix} \quad (24)$$

Known Systems with Arbitrary External Inputs

Theorem 3. Assume that $f(x, u, t)$ is bounded. Then, there exists a high-gain PI-observer for the system (2) such that $\hat{x}(t) - x(t) \rightarrow 0$ ($t > 0$) for any initial states $x(0)$, $\hat{x}(0)$ and $\hat{f}(0)$ if

1) (A, C) is observable, which includes

$$\text{rank} \left\{ \begin{bmatrix} C \\ CA \\ \vdots \\ CA^{k-1} \end{bmatrix} \right\} = n \quad , \quad (25)$$

where k is the observability index of (A, C) ,

$$\begin{aligned} 2) \text{rank} \left\{ \begin{bmatrix} A & N_1 \\ C & 0 \end{bmatrix} \right\} &= n + r_1; \text{ and} \\ 3) CN &= 0 \end{aligned}$$

Proof. Let $L_3 = N_1$. Then, analogously with the proof of Theorem 2, it is easily verified that the dynamics of PI-observer (11) for the system (2) can be arbitrarily assigned by means of the matrices L_1 and L_2 if the conditions 1) and 2) in Theorem 3 are satisfied.

Under the selection of L_3 the dynamics (13) of the estimation error becomes (20). When A_e is stable, the solution to (20) will be also bounded if $f(x, u, t)$ is bounded. Let $\begin{bmatrix} L_1 \\ L_2 \end{bmatrix} = \rho_1 \begin{bmatrix} \tilde{L}_1 \\ \tilde{L}_2 \end{bmatrix}$.

Then, (20) may be written as

$$\frac{1}{\rho_1} \begin{bmatrix} \dot{e} \\ \dot{\hat{f}} \end{bmatrix} = \frac{1}{\rho_1} \begin{bmatrix} A & N_1 \\ 0 & 0 \end{bmatrix} \begin{bmatrix} e \\ \hat{f} \end{bmatrix} - \begin{bmatrix} \tilde{L}_1 \\ \tilde{L}_2 \end{bmatrix} C e - \frac{1}{\rho_1} \begin{bmatrix} N_1 \\ 0 \end{bmatrix} f \quad (26)$$

From (26) it follows that

$$C e = 0 \quad (27)$$

for $\rho_1 \rightarrow \infty$. Differentiating (27) and using (13) give

$$C \dot{e} = C(A - L_1 C)e + CN(\hat{f} - f) \quad (28)$$

From the condition 3) and (27)

$$C A e = 0 \quad (29)$$

results.

In the same way under the condition 1) equation

$$C A^i e = 0 \quad i = 0, 1, \dots, k-1 \quad (30)$$

is obtained.

Then from (27), (29) and (30) it follows that

$$e = 0 \quad (31)$$

due to condition 1). Substituting (31) into (13) gives

$$\hat{f} - f = 0 \quad (32)$$

because of the full-column rank of N_1 . Equations (31) and (32) mean that the estimates \hat{x} and \hat{f} of the PI-observer (13) converge to the states x and the unknown inputs f of the system (2) when ρ_1 goes to the infinity. This shows that \hat{x} and \hat{f} may approximate x and f in the case of high gains.

In [9], [10] furthermore it is shown, that this type of observer also can be applied in general to systems not completely known with unknown additive inputs.

In the meantime the condition for the application of the PI-Observer to such structures is corrected to the conditions

$$\rho_1 \rightarrow \infty \quad \text{and} \quad (33)$$

$$\frac{\rho_2}{\rho_1} \rightarrow \infty \quad \text{with} \quad L_3 = \rho_2 N_1. \quad (34)$$

which gives theoretical hints to understand the observed success of the observer technique in robotics and machine-dynamics. In this application the PIO is applied to known systems with arbitrary external inputs. This concludes the understanding of the estimation behaviour of the PIO [9], [2].

THE RAIL-WHEEL CONTACT

The aim of this contribution is to demonstrate the possibilities of observer-based estimation of nonlinear contact forces. Therefore, it is not necessary to work with detailed models of the mechanical system itself rather than with arbitrary disturbed models to examine the robustness of the observer technique itself to its own model assumptions.

The modeling of the linear system part results from [?]. The complete system can be modeled without restriction for the development of the contact-force-observer as follows

$$\dot{x} = Ax + Bu + N_1 f_1 \quad (35)$$

with the state vector

$$x = \begin{bmatrix} x_1 \\ \dot{x}_1 \end{bmatrix}, \quad x_1 = \begin{bmatrix} \varphi_M \\ \varphi_{W_y} \\ u_{W_x} \\ u_{W_z} \\ u_{R1} \\ u_{R2} \end{bmatrix}, \quad (36)$$

with the motor angle φ_M , the wheel angle φ_{W_y} , the horizontal displacement of the wheelset u_{W_x} , the vertical displacement of

the wheelset u_{W_z} and u_{R1} and u_{R2} the first and the second part of the vertical displacement of the rail. The term $N_1 f_1$ represents the nonlinear system part.

This nonlinear part includes the normal force N and the tangential force T_ξ . For the determination of the tangential force the normal force and the slip v is needed. Further parts of the state vector are fed back for the computation of the normal force and the slip.

The description of the normal force N is made in dependency of the vertical displacement d [1]:

$$N = \frac{G}{2(1-\nu_Q)} \sqrt{r} \left(\frac{d}{\alpha_a} \right)^{\frac{3}{2}}, \quad (37)$$

with the wheel radius r , the shear modulus G , the contraction number ν_Q and the coefficient α_a . The vertical displacement consists of the displacements u_{R1}, u_{R2}, u_{W_z} and the disturbance height Δ [?]:

$$d = u_{R1} + u_{R2} - u_{W_z} + \Delta. \quad (38)$$

For the following simulations, Δ (as a stochastic value) works as an excitation. For $d < 0$, i.e. for a lift-off of the wheel, in the simulation d is set to zero. The values u_{R1}, u_{R2}, u_{W_z} result from the differential Eqn. (35) and (36).

From the slip-definition

$$v_\xi = \frac{\dot{\varphi}_{W_y} r - v_0}{\varphi_{W_y} r}, \quad (39)$$

with the wheel angle φ_{W_y} , the radius r and the absolute velocity of the bogie v_0 , follows with consideration of the horizontal displacement of the wheelset u_{W_x} the slip-definition

$$v_\xi = 1 - \frac{v_0}{\dot{\varphi}_{W_y} r} + \frac{\dot{u}_{W_x}}{\dot{\varphi}_{W_y} r}. \quad (40)$$

In absence of the absolute velocity of the bogie v_0 in the simulation, the following computation of the slip is applied:

$$v_\xi = 1 - \frac{\dot{\varphi}_{W_y}}{\dot{\varphi}_M} + \frac{\dot{u}_{W_x}}{r \dot{\varphi}_M}, \quad (41)$$

with the motor angle velocity $\dot{\varphi}_M$.

The tangential contact force T_ξ is modeled according to [11], as

$$T_\xi = \alpha T_{\xi, \text{lin}} = -\alpha abGC_{11} v, \quad (42)$$

with

$$\alpha = \begin{cases} 1 - \frac{1}{3} \left(\frac{T_{\xi, \text{lin}}}{\mu N} \right) + \frac{1}{27} \left(\frac{T_{\xi, \text{lin}}}{\mu N} \right)^2 & \text{for } T_{\xi, \text{lin}} < 3\mu N \\ \frac{\mu N}{T_{\xi, \text{lin}}} & \text{for } T_{\xi, \text{lin}} \geq 3\mu N \end{cases} \quad (43)$$

and C_{11} as a Kalker coefficient, which is chosen fixed. Here N is again the normal force and the friction coefficient μ is stochastically varied for the simulation.

APPLICATION OF THE OBSERVER – MEASUREMENT SLEEVE

In this section, the applicability of the observer for the above described system with a measurement sleeve is shown. With the measurement sleeve [12], the displacement between the axle and the sleeve should be determined. With this measurement-bearing, measurements in all three axle directions are possible. The advantage of the measurement in the non-rotating axle bearing is that no wiring of the rotating wheelset is needed. With the measurement values of the sleeve and the observer technique, the contact forces between the rail and the wheel should be yield. In Fig. 3 the installation position is shown.

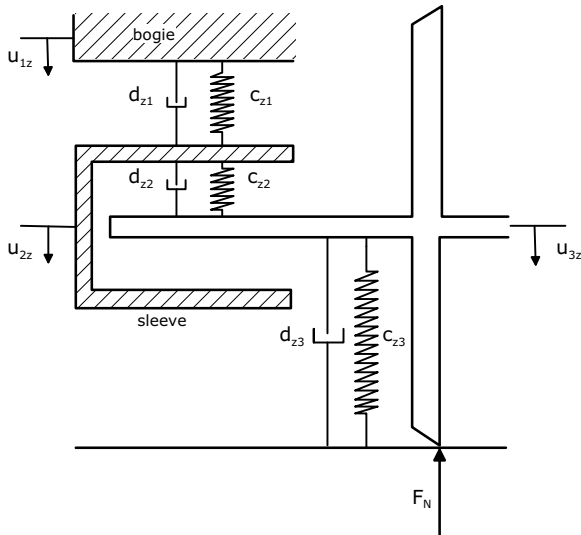


Figure 3. MODEL OF THE SLEEVE IN Z-DIRECTION

With the notations from Fig. 3 the equations of motion can be written as

$$M\ddot{u}_z = D\dot{u}_z + Cu_z + F \quad , \quad (44)$$

with

$$\begin{aligned} D &= \begin{bmatrix} -d_{z1} & d_{z1} & 0 \\ d_{z1} & -d_{z1} - d_{z2} & d_{z2} \\ 0 & d_{z2} & -d_{z2} - d_{z3} \end{bmatrix} \quad , \\ C &= \begin{bmatrix} -c_{z1} & c_{z1} & 0 \\ c_{z1} & -c_{z1} - c_{z2} & c_{z2} \\ 0 & c_{z2} & -c_{z2} - c_{z3} \end{bmatrix} \quad , \\ M &= \begin{bmatrix} m_C & 0 & 0 \\ 0 & m_H & 0 \\ 0 & 0 & m_W \end{bmatrix} \quad , \quad F = \begin{bmatrix} 0 \\ 0 \\ -F_N \end{bmatrix} \quad \text{and} \\ u_z &= \begin{bmatrix} u_{1z} \\ u_{2z} \\ u_{3z} \end{bmatrix} \quad , \end{aligned} \quad (45)$$

with the mass of the car body m_C , the mass of the sleeve m_H and the mass of the wheel and the half of the axis m_W .

In the same way, the sleeve is modeled for the x -direction, with the exception that only the third state is excluded. So that the system including the sleeve model can be brought in the form of Eqn. (2), which is needed for the observer development. From the conversions

$$u_{az} = u_{1z} - u_{2z} \quad (46)$$

$$u_{bz} = u_{2z} - u_{3z} \quad (47)$$

the measurable state u_{bz} results, which is the distance measurement given by the sleeve. For the x -direction the measurable state is $u_{bx} = u_{2x}$. With these sleeve models and the equations for $\varphi_M, \varphi_{W_y}, u_{R1}, u_{R2}$ (see Eqn. (36)) according to [?], the whole system can be written again as Eqn. (2).

The simulation model, which is used for the observer development only uses the states $\varphi_M, \varphi_{W_y}, u_{ax}, u_{bx}, u_{az}, u_{bz}$ (with u_{3z} set to zero in u_{bz}). This system given in form (2), can be brought into form (5) and (6). With the measurements u_{bx} and u_{bz} this extended system (A_e, C_e) is observable. Therefore, the observer is applicable to the estimation of the unmeasurable contact forces. Based on the linear system information, the observer is able to estimate the nonlinearity N_1 , which includes the tangential contact force T_{ξ} (x -direction) and the normal force F_N (z -direction) as shown in Fig. 4.

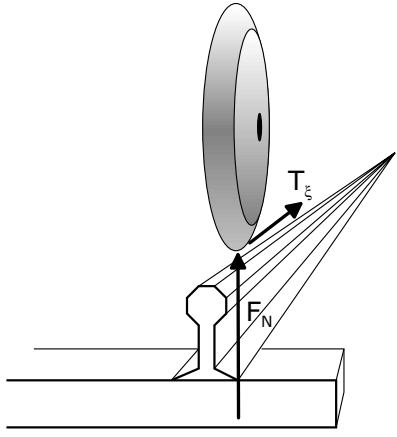


Figure 4. CONTACT FORCES

For the simulations the input is the torque $M(t)$ as a step function. Therefore a step function $M(t) = 1(t - 1s) \cdot M$ with $M = 5 \cdot 10^4$ N·m is applied. In Fig. 5 the results for the PI-Observer using the two measurements u_{bx} and u_{bz} are depicted. The upper plot shows the time behavior of the tangential contact force T_ξ and its estimation. Then the time behavior of the normal force N and its estimation are shown.

The estimation of the tangential contact force already works well, while the estimation of the normal force is only near the characteristics of the real values.

APPLICATION OF THE OBSERVER USING ACCELERATION MEASUREMENTS

The PI-Observer is shown above, in the application of the rail-wheel contact force estimation. In this example, the observer is based on displacement measurements. Now, the applicability of this observer scheme in the case of acceleration measurements is shown here for the first time. The basic idea is to replace the displacement sensors of the measurement sleeve by low-cost accelerometers. Here, the shown approach to estimate contact forces is reformulated to the use of accelerometers for the first time. To show the principle, the example of the contact force estimation of an elastic beam is used for first considerations.

The observer development starts again with the system description

$$\dot{x} = Ax + Bu + N_1 f(x, u, t) \quad \text{with} \quad x = \begin{bmatrix} x_1 \\ \dot{x}_1 \end{bmatrix}. \quad (48)$$

The output includes only accelerations. With an output matrix C

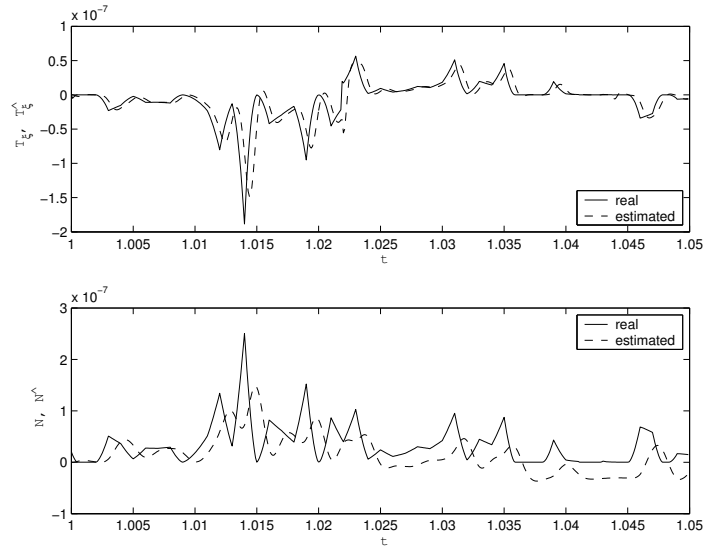


Figure 5. SIMULATION OF THE RAIL-WHEEL CONTACT USING MEASUREMENTS FROM THE AXLE SLEEVE

given by $C = [0 \quad C^*]$ the output is

$$y = C\dot{x} = [0 \quad C^*] \begin{bmatrix} \dot{x}_1 \\ \ddot{x}_1 \end{bmatrix} = C^* \ddot{x}_1, \quad (49)$$

i.e. from the derivative of the state vector only selected values of the second part are appearing at the output. These are exactly the accelerations.

Then the observer is built for the system

$$\dot{x} = Ax + B\dot{u} + Nf^*(x, u, t) \quad \text{with} \quad f^* = \dot{f}. \quad (50)$$

The nonlinearities are again approximated by

$$f^* \approx H v_1, \quad (51)$$

whereby v_1 is described (based on [6]) as

$$\dot{v} = Fv \quad \text{with} \quad v = \begin{bmatrix} v_1 \\ \dot{v}_1 \end{bmatrix}, \quad (52)$$

Then the observer for the extended system

$$\begin{bmatrix} \dot{\hat{x}} \\ \dot{\hat{v}} \end{bmatrix} = \begin{bmatrix} A & NH \\ 0 & F \end{bmatrix} \begin{bmatrix} \hat{x} \\ \hat{v} \end{bmatrix} + \begin{bmatrix} B \\ 0 \end{bmatrix} \dot{u}, \quad (53)$$

$$y = [C \quad 0] \begin{bmatrix} \hat{x} \\ \hat{v} \end{bmatrix}, \quad (54)$$

can be built analog to (11). The use of the introduced observer technique now follows the same ideas as shown in Eqn. (12)-(33). It estimates \hat{v} and therewith \hat{f}^* so that $\hat{f} = \int \hat{f}^*$ can be determined.

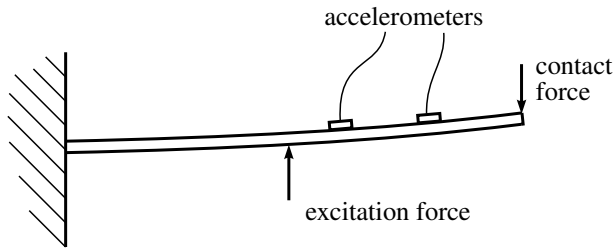


Figure 6. FLEXIBLE BEAM

As an example for this new approach a one side fixed beam model is used. This application of the estimation with the aid of acceleration measurements is used as a first simulation example. In the future, the transformation and expansion to the problem of the rail-wheel contact will be realized.

The beam is modeled using 5 finite beam elements. Caused by an excitation force, a contact at the end of the beam results in a contact force F . This high-frequency contact characteristic is estimated by the PI-Observer based on acceleration measurements at two nodes. In Fig. 6, a schematic representation of the beam is shown.

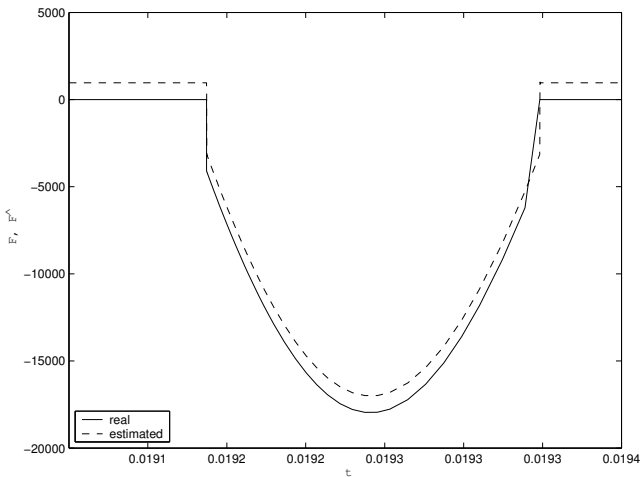


Figure 7. SIMULATION OF THE BEAM WITH ACCELERATION MEASUREMENTS

The result of the comparison of the original value F with the estimated value \hat{F} is shown in Fig. 7. It displays the possibility of detecting the peak of the contact force. The problem left by this procedure is a deviation of the amplitude, which will be examined in the future work.

CONCLUSIONS AND OUTLOOK

This contribution shows the scheme of the ‘virtual measurement device’ using the PI-Observer for the reconstruction of unmeasurable forces. After the introduction of this observer the modeling of the rail-wheel contact and the measurement sleeve is shown. With the simulation of the dynamic behavior of the axle bearing, the applicability of this scheme for the rail-wheel contact force determination is pointed out. Here the tangential contact force and the normal force were estimated by using displacement measurements.

Further the idea of using the PI-Observer with acceleration measurements is shown. As an example the time behaviour of the contact force of an elastic beam was reconstructed.

After improving this observer technique this scheme should be used for the validation of the rail-wheel contact behaviour. Further applications for the PI-Observer could be the control of single wheel-drives.

ACKNOWLEDGMENT

This work is part of the project ‘Observer-Based Validation of the Rail-Wheel Contact’ as a part of the German Research Council (DFG) Priority-Program ‘System Dynamics and Long-Term Behavior of Vehicle, Track and Subgrade’. The authors wish to express their thanks to the DFG for the support.

REFERENCES

- [1] Ripke, B., 1995. ”Hochfrequente Gleismodellierung und Simulation der Fahrzeug-Gleis-Dynamik unter Verwendung einer nichtlinearen Kontaktmechanik”. In *VDI-Fortschrittberichte*, Reihe 12, Nr. 249, Düsseldorf.
- [2] Söffker, D., 1999. ”Observer-based measurement of contact forces of the nonlinear rail-wheel contact as a base for advanced traction control”. In *Mechatronics and Advanced Motion Control*, Wallaschek, J., Lückel, J., and Littmann, W., (eds.), vol. 49. HNI-Verlagsschriftenreihe, pp. 305–320.
- [3] Söffker, D., Bajkowski, J., and Müller, P.C., 1993. ”Crack Detection in Turbo Rotors – A New Observer - Based Method”. In *ASME Journal of Dynamic Systems, Measurements, and Control*, vol. 3, pp. 518 - 524.
- [4] Ackermann, J., 1989. ”Positionsregelung reibungs-behafteter elastischer Industrieroboter”. In *VDI-*

- Fortschrittberichte*, Reihe 8, Nr. 180, VDI-Verlag, Düsseldorf.
- [5] Neumann, R. and Moritz, W., 1990. "Observer-based joint controller design for a robot for space operation". In *Proc. Eight CISM-IFTOMM Symp. Theory of Robots and Manipulators*, Ro.Man.Sy.
 - [6] Johnson, C.D., 1976. "Theory of Disturbance-Accommodating Controllers". In *Control and Dynamic Systems*, Ed. C.T.Leondes, vol. 12. Academic Press, pp. 387-489.
 - [7] Müller, P.C. and Lückel, J., 1977. "Zur Theorie der Störgrößenaufschaltung in linearen Mehrgrößenregelsystemen". In *Regelungstechnik*, vol. 25, pp. 54-59.
 - [8] Müller, P.C., 1998. "Indirect Measurement of Nonlinear Effects by State Observer", In *IUTAM Symposium on Nonlinear Dynamics in Engineering Systems*, University of Stuttgart, FRG.
 - [9] Söffker, D., Yu, T.J. and Müller, P.C., 1995. "State Estimation of Dynamical Systems with Nonlinearities by using Proportional-Integral Observer". *International Journal of Systems Science*, **26**(9), pp.1571–1582.
 - [10] Söffker, D., 1996. "Zur Modellbildung und Regelung längenvariabler, elastischer Roboterarme", In *VDI-Fortschrittberichte*, Reihe 8, Nr. 584. VDI-Verlag, Düsseldorf. Dissertation, Bergische Universität Wuppertal, 1995.
 - [11] Shen, Z.Y., Hedrick, J.K. and Elkins, J.A., 1983. "A comparison of alternative creep force models for rail vehicle dynamic analysis", In *Proc. of 8th IASVD Symposium*, MIT, Cambridge, August 15–19.
 - [12] Meinke, P., Meinke, S. and Blenkle, C., 2001. "Nichtlinearitätensensor für den Laufzustand von Radsätzen". In *Detection, Utilization and Avoidance of Nonlinear Dynamical Effects in Engineering Applications*, Ed. K. Popp, Berichte aus der Physik. Shaker Verlag, Aachen, pp. 131-154. Final Report of a Joint Research Project Sponsored by the German Federal Ministry of Education and Research.